Journal of Power Sources 185 (2008) 85–94

Contents lists available at ScienceDirect

Journal of Power Sources

journal homepage: www.elsevier.com/locate/jpowsour

Proton conducting membranes prepared by incorporation of organophosphorus acids into alcohol barrier polymers for direct methanol fuel cells

Zhongyi Jiang, Xiaohong Zheng, Hong Wu*, Fusheng Pan

Key Laboratory for Green Chemical Technology, School of Chemical Engineering and Technology, Tianjin University, Tianjin 300072, China

ARTICLE INFO

Article history:
Received 23 May 2008
Received in revised form 26 June 2008
Accepted 26 June 2008
Available online 11 July 2008

Keywords:
Organophosphorus acid
PVA
Chitosan
Proton conductivity
Methanol permeability

ABSTRACT

A novel type of DMFC membrane was developed via incorporation of organophosphorus acids (OPAs) into alcohol barrier materials (polyvinyl alcohol/chitosan, PVA/CS) to simultaneously acquire high proton conductivity and low methanol permeability. Three kinds of OPAs including amino trimethylene phosphonic acid (ATMP), ethylene diamine tetra(methylene phosphonic acid) (EDTMP) and hexamethylene diamine tetra(methylene phosphonic acid) (HDTMP), with different molecular structure and phosphonic acid groups content were added into PVA/CS blends and served the dual functions as proton conductor as well as crosslinker. The as-prepared OPA-doped PVA/CS membranes exhibited remarkably enhanced proton conducting ability, 2–4 times higher than that of the pristine PVA/CS membrane, comparable with that for Nafion® 117 membrane (5.04×10^{-2} S cm^{-1}). The highest proton conductivities 3.58×10^{-2}, 3.51×10^{-2} and 2.61×10^{-2} S cm^{-1} for ATMP-, EDTMP- and HDTMP-doped membranes, respectively were all achieved at highest initial OPA doping content (23.1 wt.%) at room temperature. The EDTMP-doped PVA/CS membrane with an acid content of 13.9 wt.% showed the lowest methanol permeability of 2.32×10^{-7} cm^2 s^{-1} which was 16 times lower than that of Nafion® 117 membrane. In addition, the thermal stability and oxidative durability were both significantly improved by the incorporation of OPAs in comparison with pristine PVA/CS membranes.

1. Introduction

The proton-exchange membrane (PEM) is a key component in DMFCs, which directly determines the final fuel cell performance. Membranes with high proton conductivity and low methanol permeability as well as high stability have always been the targets for membrane development [1]. In recent years, a large number of sulfonated membranes have been synthesized through various methods including direct sulfonation of aromatic polymers [2,3], grafting of branches with sulfonic acid groups [4,5] and blending of different sulfonated polymers or blending of sulfonated polymers with basic polymers [6,7]. The proton conductivity of these sulfonated membranes strongly depends on the water content since the protons transport with the aid of water as mobile vehicles. Nafion® 117 membrane, currently the major type of commercially available membrane for DMFC and a typical representative of sulfonated membranes, displays a sharp decrease in proton conductivity at operation temperatures higher than 80 °C due to a big loss of water content [8]. Additionally, the high water content in the membrane usually leads to a high methanol crossover and consequently a lowered fuel cell performance. An effective alternative approach to eliminate this water dependence for sulfonic acid membranes is to use phosphonic acids as proton conductors. The water binding energy of phosphonic acid (47.3 kJ mol^{-1}) was found to be higher than that of sulfonic acid (44.4 kJ mol^{-1}) [9], suggesting that the phosphonic acid group has a better capacity of retaining water under low-humidity conditions and that the dynamics of the hydrogen bonding is more constrained with $-PO_3H_2$ than $-SO_3H$. The proton transport through phosphonic acid membranes under low-humidity conditions is fulfilled via diffusion along hydrogen bonds [10–12]. The average zero point energy (ZPE) corrected energy difference for phosphonic acid and sulfonic acid was 37.2 and 69.9 kJ mol^{-1}, respectively, indicating that protons transport much easier from 'acid to acid' via phosphonic acid groups than via sulfonic acid groups [9].

The most commonly applied approach to introduce an inorganic acid into polymer membranes is by direct doping [12–14]. The proton conductivity can be significantly increased after doped with H_3PO_4 [15] and other heteropolyacids [16,17]. However, a quick leaching of the small inorganic acids from the membrane, especially when contacting with liquid fuels, often occurs for such kind of acid-doped membranes [13,15,18]. The leaching of acids not only

* Corresponding author. Tel.: +86 22 27892143; fax: +86 22 27892143.
E-mail address: wuhong2000@gmail.com (H. Wu).

0378-7753/$ – see front matter © 2008 Elsevier B.V. All rights reserved.
doi:10.1016/j.jpowsour.2008.06.086

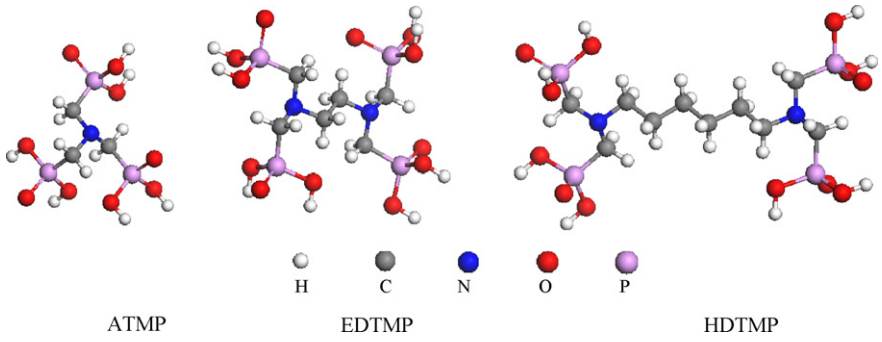

Scheme 1. Molecular structure of ATMP, EDTMP and HDTMP.

results in a fast decrease of conductivity, but also causes corrosion problems. In order to address this problem, synthesis of phosphonic acid membranes through chemical modifications of polymers was introduced to be the most effective method [10,11,19–21]. Proton conductivity of phosphonic acid membranes is directly associated with the degree of phosphonation. A higher density of phosphonic acid groups in the membrane leads to a higher proton conductivity [21]. The disadvantages of the relatively complicated procedure for fabrication of chemically modified membranes and the leaching problem for physical doping membranes promote the development of novel and simple approaches.

Herein, organophosphorus acids (OPAs) are for the first time incorporated into alcohol barrier polymers, polyvinyl alcohol (PVA) and chitosan (CS), by solution blending. OPA, used as a proton conductor, is such a kind of phosphonic acid with a couple of $-PO_3H_2$ groups at the both ends of the alkyl chain. On the one hand, the $-PO_3H_2$ groups on the both chain ends may act as crosslinking sites by forming ionic bonds or hydrogen bonds with polymers like CS with $-NH_2$ groups. On the other hand, the high content of $-PO_3H_2$ group on the OPAs is expected to yield high proton conductivity, which is less dependent on water uptake. Three different OPAs including amino trimethylene phosphonic acid (ATMP), ethylene diamine tetra(methylene phosphonic acid) (EDTMP) and hexamethylene diamine tetra(methylene phosphonic acid) (HDTMP) are selected and their molecular structures are shown in Scheme 1. ATMP, EDTMP and HDTMP with different $-(CH_2)_n-$ chain length (n = 0, 2, or 6) present an equivalent acid density of 9.93, 9.09 and 8.06 mmol $(-PO_3H_2)\,g^{-1}$, respectively. ATMP is soluble in aqueous solution, while EDTMP and HDTMP are insoluble in water but soluble in ammonia aqueous solution at room temperature. Taking reducing methanol permeation, film-forming property and manufacturing cost into account, blends of PVA and CS are selected as the polymer matrix [22–24].

2. Experimental

2.1. Materials and chemicals

PVA with an average degree of polymerization of 1750 ± 50 was purchased from Tianjin Yuanli Chemical Co., Ltd. CS with a degree of deacetylation of 90% was supplied by Zhejiang Golden-Shell Biochemical Co., Ltd. ATMP, EDTMP and HDTMP were purchased from Shandong Taihe Water Treatment Co., Ltd. Formic acid, acetone, glutaraldehyde (GA) and methanol were purchased locally. Distilled water was used throughout the study.

2.2. Membrane preparation

OPA-doped PVA/CS membranes with various OPA contents were prepared through solution blending. A PVA solution with a concentration of 4 wt.% was prepared by dissolving the PVA powder in de-ionized water at 90 °C under stirring for 2 h. CS was dissolved in a 4 wt.% formic acid aqueous solution at 80 °C under stirring to get a 4 wt.% homogeneous CS solution. Then, the PVA solution and the CS solution were mixed at a ratio of 1:1 and a homogeneous blend solution was obtained. A desired amount of OPA (ATMP, EDTMP or HDTMP) was added to the above polymer solution under constant stirring for 1 h. A small amount of GA (1–59 mol of PVA repeat units) was used for primary crosslinking. The mixture was then cast on a clean glass plate and dried at room temperature for about 36 h. The resultant membranes were further treated in a vacuum at 120 °C for 1 h. Then the dry membranes were equilibrated in water for about 30 min followed by immersing in an acetone–water (90/10, vol.%) solution containing 0.5 vol.% of HCl as a catalyst and 5 vol.% of GA for further crosslinking. After crosslinking for 30 min, the membranes were rinsed repeatedly with distilled water to remove traces of unreacted GA in the membrane before being dried in a vacuum oven at 120 °C for another 30 min. The membrane thus fabricated was designed as PVA/CS-X(Y), where X (X = A, E or H) indicated the type of the OPA, A standing for ATMP, E standing for EDTMP and H standing for HDTMP, and Y was the actual weight percent of the OPA in the membrane. The actual content of OPA in the membrane was determined by titration method. The membranes without further crosslinking by GA were immersed in distilled water and the water was change repeatedly until a neutral pH value was reached. The aqueous solution with leached OPAs was then titrated with a 0.01 M NaOH solution using phenolphthalein as an indicator. The content of OPAs in the membrane was calculated based on the total amount added and the amount leaching out of the membrane.

Pure PVA membrane was also prepared for comparison purpose. A PVA solution (4 wt.%) was prepared by dissolving preweighed PVA powder in water at 90 °C under stirring for 2 h. A 2.5 wt.% GA solution was added dropwisely to the above PVA solution, and HCl was added as a catalyst. The solution was then cast on a clean glass plate and dried at room temperature for about 36 h. Then the treatment of PVA membrane was the same with OPA-doped membranes.

2.3. Characterizations

2.3.1. Fourier transform infrared (FT-IR)

The chemical structure of the PVA/CS and OPA-doped PVA/CS membranes was investigated using a Nicolet-740, PerkinElmer-283B FT-IR Spectrometer.

2.3.2. X-ray photoelectron spectroscopy (XPS)

XPS measurements were performed on a PHI 1600 spectrometer with a Mg Kα radiation for excitation to analyze the element existing status of nitrogen on the membrane surface.

Table 1
Calculated hydrogen bond and electrostatic energies for PVA/CS-E, PVA/CS, and EDTMP

Energy	E_{total} (kJ mol^{-1})	$E_{PVA/CS}$ (kJ mol^{-1})	E_{EDTMP} (kJ mol^{-1})	ΔE (kJ mol^{-1})
Hydrogen bond	−2451.452	−2041.780	−26.153	−383.519
Electrostatic	−10084.372	−3372.062	−515.529	−6196.781

2.3.3. X-ray diffraction (XRD)

The crystallinity of the membranes was investigated with a RigakuD/max2500v/pa X-ray diffractometer (CuK 40 kV, 200 mA, 2°min^{-1}). The peak position and its area were extracted with MDI-jade5 software [25].

2.3.4. Thermal analysis

The thermal stability of the membranes was studied using thermal gravimetric analysis with a SHIMADZU TA-50 instrument under an air atmosphere at a heating rate of 10 °C min^{-1}. All the membrane samples were stored in a vacuum oven at 100 °C before analysis.

2.3.5. Mechanical property

The tensile strength of the blend membranes was measured at room temperature using an Instron-type tensile testing machine (Testometric/M350-10KN ROCHOALL, England) at a crosshead speed of 1 mm min^{-1}. The width of the sample was 10 mm and the length between the jaws was 30 mm. All the measurement was performed at 25 ± 2% relative humidity (RH).

2.4. Oxidation experiments

The oxidation resistance of the membranes was evaluated by immersing the samples in a 3 wt.% H_2O_2 aqueous solution with stirring at 60 °C for 7 days. The weight loss of the membranes was measured at certain time intervals.

2.5. Water uptake

The water uptake of the membranes was determined by measuring the membrane weight difference before and after immersion in water for 24 h. The membrane was wiped with a filter paper to remove the water on the surface and weighted (W_{wet}). Then the membrane sample was dried in a vacuum oven at 60 °C for 24 h and weighted (W_{dry}). The water uptake was calculated using Eq. (1).

$$\text{Uptake (wt.\%)} = \frac{W_{wet} - W_{dry}}{W_{dry}} \times 100 \quad (1)$$

The error of measurements was within ±4%.

2.6. Ion-exchange capacity (IEC)

The IEC of the membranes was measured by a conventional titration method. The membrane in H^+ form was immersed in a 2 M NaCl solution for 24 h to replace the H^+ with Na^+ completely. The remaining solution was then titrated with a 0.01-M NaOH solution using phenolphthalein as an indicator. The IEC value was calculated by Eq. (2).

$$\text{IEC(mmol g}^{-1}) = \frac{0.01 \times 1000 \times V_{NaOH}}{W_d} \quad (2)$$

where V_{NaOH} (L) is the volume of NaOH solution consumed for titration and W_d (g) is the weight of the dry membrane sample. The measurements were carried out with an accuracy of 0.001 mmol g^{-1}.

2.7. Proton conductivity

The proton conductivity of the membranes was measured in a two-point-probe conductivity cell using the AC impedance spectroscopy method as described in Ref. [25]. A frequency response analyzer (FRA, Autolab PGSTST20) over a frequency range of 1–10^6 Hz with an oscillating voltage of 10 mV was used to measure the membrane impedance. The test temperature was controlled by the water vapor from room temperature to 80 °C. Before measurement, the membrane was equilibrated in de-ionized water for 24 h.

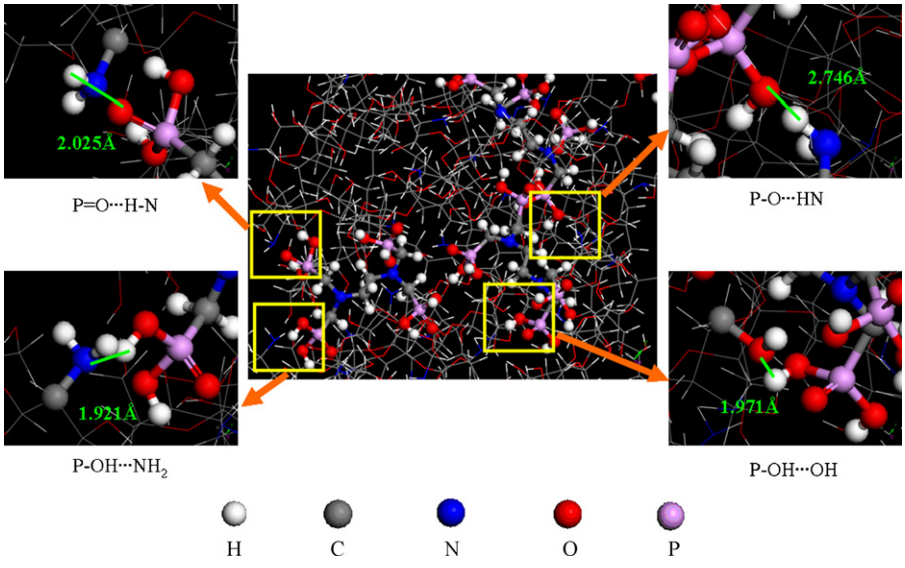

Fig. 1. Optimized structure of EDTMP-doped PVA/CS blend.

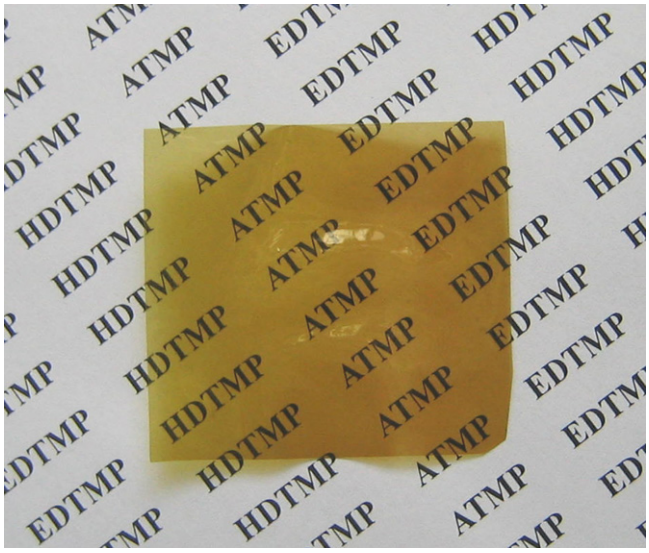

Fig. 2. A representative photograph of the OPA-doped PVA/CS blend membranes.

The proton conductivity of the membrane was calculated by Eq. (3).

$$\sigma(\mathrm{S\ cm^{-1}}) = \frac{L}{AR} \tag{3}$$

where L (cm) is the distance between the two probes; A (cm^2) is the cross-sectional area of testing sample; and R (Ω) is the membrane resistance derived from the low intersection of the high frequency semicircle on a complex impedance plane with the *Re* (Z) axis.

2.8. Methanol permeability

The methanol permeability was measured using a diffusion cell as described in Ref. [25]. The membrane was full hydrated in de-ionized water for 48 h before measurement. A 5 M methanol solution was used as the feed. A gas chromatography (Agilent 6820) equipped with a TCD detector and a DB624 column was used to detect the change of methanol concentration in the water compartment. The methanol

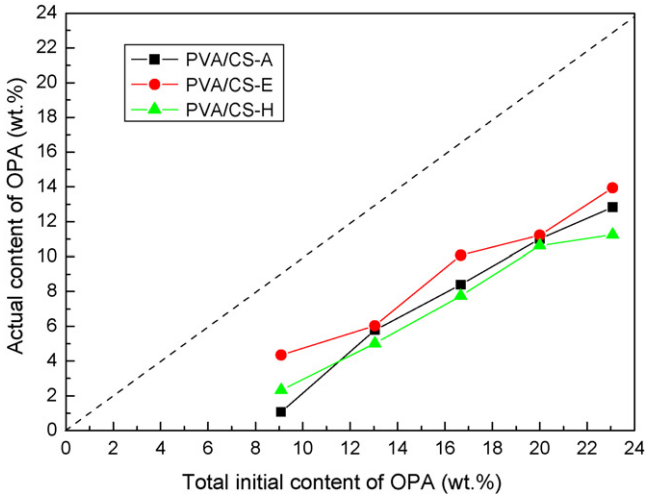

Fig. 3. Actual content of OPAs *vs.* total initial content of OPAs in blend membranes (the dash line is the diagonal line).

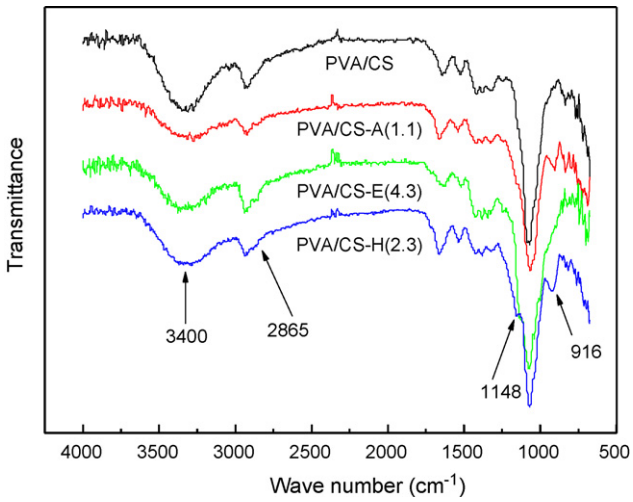

Fig. 4. FT-IR spectra of PVA/CS and OPA-doped PVA/CS membranes.

permeability (P, $cm^2\ s^{-1}$) was determined by Eq. (4).

$$P(\mathrm{cm^2\ s^{-1}}) = \frac{SV_B L}{AC_{A0}} \tag{4}$$

where S is the slope of curve of concentration change *vs.* time; V_B is the volume of the water compartment; C_{A0} is the initial methanol concentration; L and A are the thickness and area of the membrane, respectively. The error of measurements was within ±3%.

3. Results and discussion

3.1. Calculations of interaction energy in the blend membrane

Membrane performance is strongly dependent on its equilibrium conformational structure. Recently, molecular dynamics simulation method has been applied in the design and selection of membrane materials for different separation processes, and proven to be a useful tool for the investigation of the structure and molecular interactions in the target membranes [26]. Herein, a primary simulation was conducted, hoping to provide a basis for understanding the interactions between OPA and PVA/CS blends at molecular level. EDTMP-doped blend membrane was studied as a model system.

Molecular dynamics simulations were carried out using the Discover and Amorphous Cell module of Materials Studio, which was developed by Accelrys Software Inc. The COMPASS force field was used throughout the simulation except for the calculation of interaction energy between OPA and PVA/CS polymers since it could not provide the exact value of hydrogen bonding energy. The DREIDING force filed was used as a complement. The initial PVA and CS chains were consisted of 100 and 28 repeat units, respectively. The packing models of OPA-doped PVA/CS membrane were constructed containing two PVA chains, two CS chains and a certain amount of EDTMP molecules. The details of optimized procedure were described in Ref. [27].

The interaction energy (ΔE) between EDTMP and PVA/CS blend was calculated as follows:

$$\Delta E = E_{\mathrm{total}} - E_{\mathrm{PVA/CS}} - E_{\mathrm{EDTMP}} \tag{5}$$

where E_{total} was the potential energy of EDTMP-doped PVA/CS system, $E_{\mathrm{PVA/CS}}$ and E_{EDTMP} were the potential energy of the optimized PVA/CS blend polymer and EDTMP, respectively.

Hydrogen bond and electrostatic energies, which corresponded to the strength of interactions in the EDTMP-doped PVA/CS blend,

Table 2
N contents on the surface of PVA/CS, PVA/CS-E(4.3) without and with further crosslinking by GA

Membrane	Experimental (%)		Theoretical[a] (%)		Theoretical[b] (%)	
	N1	N2	N1	N2	N1	N2
PVA/CS	81.6	19.4	100.0	–	100	–
PVA/CS-E(4.3) (without GA)	64.3	35.7	93.6	6.4	61.4	38.6
PVA/CS-E(4.3) (with GA)	66.6	33.4	93.6	6.4	61.4	38.6

[a] Ignoring any ionic interactions between OPA and chitosan.
[b] Considering a complete ionic interaction between OPA and chitosan.

were calculated and listed in Table 1. The negative hydrogen bond energy change for the formation of complex of EDTMP and PVA/CS ($-383.519\,kJ\,mol^{-1}$) indicated that the addition of EDTMP decreased the energy of the blend system. The number of hydrogen bond (446) in EDTMP-doped PVA/CS blend was divided into two kinds: (1) the number of intra-hydrogen bond between PVA and CS was 377, which was lower than that in pristine PVA/CS blend (408), (2) and the number of inter-hydrogen bond between EDTMP and PVA/CS blend was 69. On one hand, EDTMP destroyed to some extent the original hydrogen bonds in the pristine PVA/CS blend. On the other hand, the addition of EDTMP resulted in new hydrogen bonds including P=O···HN, P–OH···NH_2, P–OH···OH and P–O···HN as shown in Fig. 1. The significant reduction in the electrostatic interaction energy after doping of EDTMP ($-6196.781\,kJ\,mol^{-1}$) compared with that for pristine PVA/CS blend ($-3372.062\,kJ\,mol^{-1}$) and EDTMP ($-515.529\,kJ\,mol^{-1}$) suggested a strong electrostatic interaction between PVA/CS blend and EDTMP. This electrostatic interaction was attributed to the acid–base interaction between the $-PO_3H_2$ groups of EDTMP and the $-NH_2$ groups of CS. These newly formed hydrogen bonds and electrostatic interactions altered the pristine crystalline structure in PVA/CS blends by presenting a compressed crosslinked structure, which was favorable for decreasing methanol crossover.

The above primary simulation results revealed the potential influence of OPA on the membrane structure. Deeper understanding and confirmation of this influence need further experimental characterization and evaluation.

3.2. Membrane preparation

A series of transparent and flexible OPA-doped PVA/CS blend membranes with a thickness of 100–115 μm were prepared. Fig. 2 shows the appearance of the blend membranes. The content of ATMP, EDTMP and HDTMP added into the PVA/CS solution was kept up to 23.1 wt.%. While ATMP is easy to dissolve in water, EDTMP and HDTMP have a solubility limit of 5% in water but easy to dissolve in ammonia aqueous solution. The presence of CS in the blends enhanced the solubility of EDTMP and HDTMP due to its basic $-NH_2$ groups. When the content of the OPAs exceeded 23.1 wt.%, an obvious phase separation occurred during the formation of membrane, and small OPAs crystals were found to crystallize out of the membrane matrix during the gradual evaporation of solvent.

3.3. OPA content in blend membranes

Since some leaching occurred during immersion before further crosslinking, the actual content of OPAs in the final blend mem-

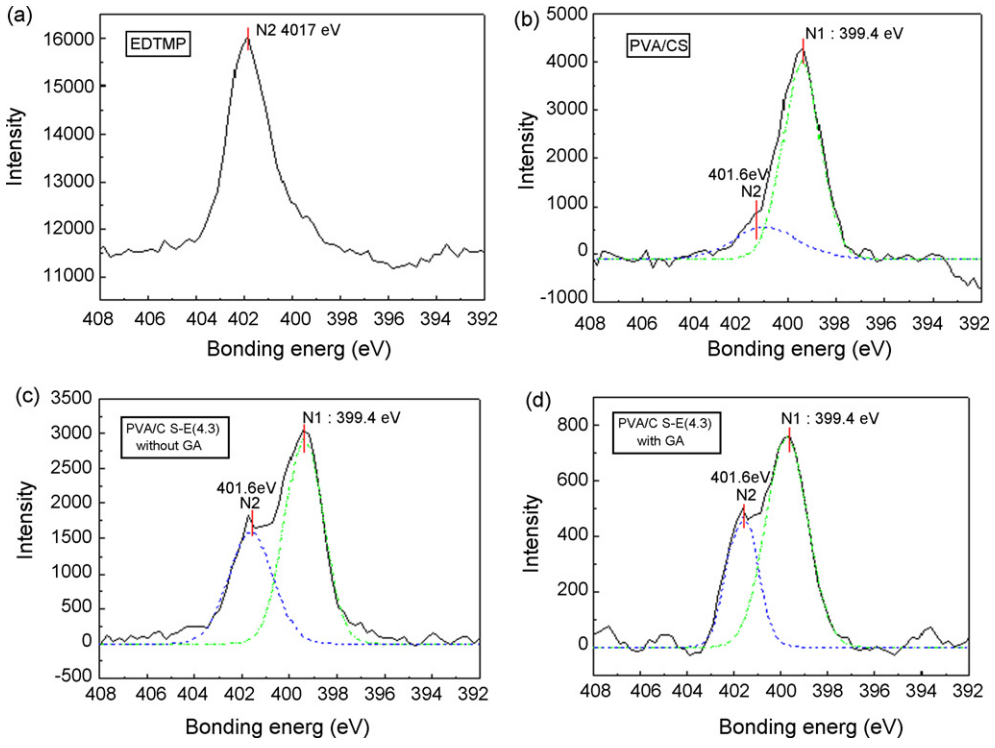

Fig. 5. High-resolution XPS spectra of N 1s for (a) EDTMP, (b) PVA/CS membrane, (c) PVA/CS-E(4.3) without and (d) with further crosslinking by GA.

branes was lower than the total initial amount added. Fig. 3 shows the actual content of OPA in blend membranes corresponding to the total initial content added. It was found that about 50% or higher percent of the OPAs was lost during the preparation procedure, and more EDTMP could be retained in the membrane than ATMP and HDTMP. The high content of phosphonic acid group (4 in one molecule) and the moderate chain length ($-(CH_2)_n-$, $n=2$) of EDTMP contributed to a stronger interaction with polymers, resulting in a stronger crosslinking effect. Little leaching of OPAs from the final membranes was found during tests of proton conductivity and methanol permeability. The contents of OPAs in the resultant blend membranes were thus expressed in their actual contents.

3.4. FT-IR spectra

FT-IR spectra of PVA/CS and OPA-doped PVA/CS membranes were shown in Fig. 4. The strong and broad band at around 3400 cm^{-1} in pure PVA/CS membrane spectra corresponded to the O–H stretching vibrations of hydroxyl groups. The intensity of this broad band decreased upon the addition of OPAs, indicating that part of the –OH groups was involved in the condensation reaction with –CHO groups of GA, forming a covalently crosslinked network. The band appeared at 1000–1100 cm^{-1} were assigned to the C–O stretching. The appearance of bands at 916, 1148, and 2865 cm^{-1} in OPA-doped membranes was attributed to the stretching of P=O and P–OH in OPAs. Furthermore, the bands at 945 and 2947 cm^{-1} for pure OPAs (spectra not shown) shifted to lower frequencies, 916 and 2865 cm^{-1}, for OPA-doped PVA/CS membranes, revealing the enhanced intermolecular hydrogen bonds formed between the acidic hydrogen atoms of OPAs and the basic amine groups and oxygen atoms on the polymer chains.

3.5. XPS analysis

The high-resolution N 1s core-level XPS spectra for EDTMP (a), PVA/CS membrane (b), PVA/CS-E(4.3) without (c) and with further crosslinking by GA (d) were presented in Fig. 5. The single peak at a bonding energy of 401.7 eV for EDTMP was attributed to the *tert*-amine (–N=) denoted as N2. In the XPS spectra of the pristine and OPA-doped PVA/CS blend membranes, two distinguishable species were resolved according to the different states of nitrogen atoms in different microenvironments. The strong peak at around 399.4 eV was assigned to the N in the amino groups ($-NH_2$) of CS (denoted as N1). In order to quantify the relative contents of N1 and N2 in the membranes, peak fittings of the N 1s XPS spectra for undoped PVA/CS membrane (Fig. 5(b)) and PVA/CS-E(4.3) membranes (Fig. 5(c) and (d)) were conducted. The peak at around 401.6 eV was attributed to the protonated amino groups ($-NH_3^+$) and the *tert*-amines (–N=) existed in the blend membranes. The contents of N1 and N2 species measured by XPS were listed in Table 2. Two kinds of theoretical content values for different N species were also calculated and listed in Table 2 for comparison, taking either no ionic interactions or a complete ionic interaction between OPAs and CS into account. For PVA/CS-E(4.3) membranes, the slight decrease in N2 content after further GA crosslinking indicated a slight influence of GA on the protonation of amine groups. The measured content of N2 (33.4%) was much higher than the theoretical value (6.4%) ignoring any interactions, but quite similar with the theoretical value (38.6%) considering a complete ionic interaction between the $-NH_2$ groups of CS and $-PO_3H_2$ groups of EDTMP. This approximation confirmed the existence of strong interactions between the OPAs and the polymers. The N2 content originated from both the amino groups ($-NH_3^+$) on CS and the *tert*-amines (–N=) on EDTMP. If the contribution of the –N= on

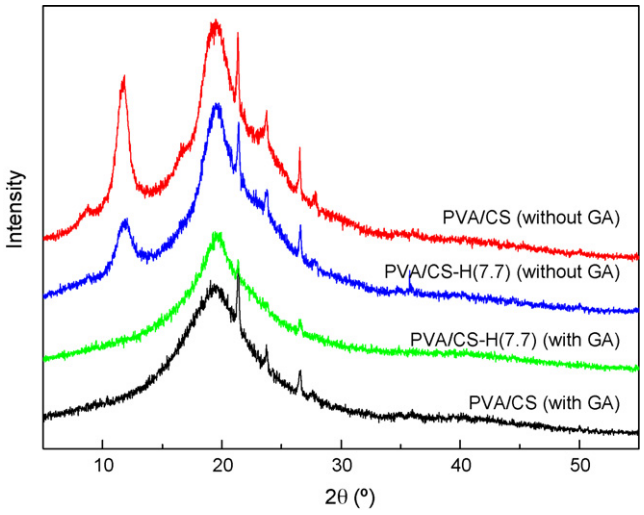

Fig. 6. XRD patterns of PVA/CS and PVA/CS-H(7.7) membranes without and with further crosslinking by GA.

EDTMP was deducted according to its doping amount, the content of N2 in protonated amino form was about 29.3% and 27.0% for the PVA/CS-E(4.3) membrane without and with GA crosslinking, respectively. These content values were much higher than that of pure PVA/CS membrane (19.4%), suggesting an enhanced protonation tendency of the amine groups with the addition of strong acids.

3.6. XRD patterns

PVA/CS-H(7.7) as a representative OPA-doped membrane was used in XRD analysis. XRD patterns of PVA/CS and PVA/CS-H(7.7) membranes without and with further crosslinking by GA are shown in Fig. 6. For the pure PVA/CS membrane without GA crosslinking, the characteristic crystalline peaks at 11.6°, 18.3°, 23.7° and 26.5° which were attributable to CS [28] and the peaks around 20° which was attributable to PVA could be clearly observed [29]. The major crystalline peak of CS at 11.6° was remarkably weakened after incorporation of HDTMP and completely disappeared after GA-crosslinking treatment, while another major peak at 18.3° was also diminished. The reduction of crystalline degree of the blend membranes was partly attributed to the

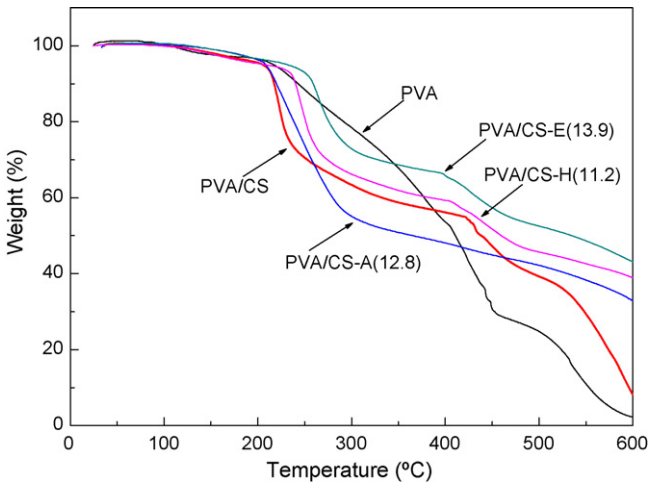

Fig. 7. TGA curves of PVA, PVA/CS and OPA-doped PVA/CS membranes.

Table 3
$T_{d\text{-onset}}$, $T_{d\text{-max}}$ and corresponding weight loss of PVA, PVA/CS and OPA-doped PVA/CS membranes

Membrane	$T_{d1\text{-onset}}$	$T_{d1\text{-max}}$	Weight loss (%)	$T_{d2\text{-onset}}$	$T_{d2\text{-max}}$	Weight loss (wt.%)
PVA	207	–	75	493	532	25
PVA/CS	212	223	35	430	441	18
PVA/CS-A(12.8)	215	250	46	–	–	14
PVA/CS-E(13.9)	246	264	24	397	425	18
PVA/CS-H(11.2)	230	244	28	402	440	18

interaction between the $-PO_3H_2$ groups on HDTMP molecules and the $-NH_2$ groups on CS chains, and partly attributed to the crosslinking reaction between the –CHO groups on GA and the –OH groups on PVA and CS. The total crystallinity of PVA/CS blend membrane was reduced from 13.4% to 10.2% by incorporation of 7.7 wt.% of HDTMP, and this value was further notably decreased to 1.5% after GA crosslinking treatment. This change in crystalline property indicated that HDTMP acting not only as an acidic additive but also as a crosslinker, interfered the packing of polymer chains by forming hydrogen bonds and ionic bonds. The decrease of crystallinity suggested an increase in amorphous phases in the membrane, which is favorable for proton transport as a result of an enhanced segmental motion of polymer chains. The change in the OPA-doped membrane structure will subsequently lead to a change in membrane performance. The reduction in crystallinity was supposed to benefit the transport of protons without a big compensation of alcohol barrier property by forming a dense crosslinked structure instead of the pristine crystalline structure.

3.7. Thermal stability

The thermal stability of PVA, PVA/CS and OPA-doped PVA/CS membranes was investigated by TGA measurement from room temperature to 600 °C in air. The TGA curves are shown in Fig. 7. The onset decomposition temperature ($T_{d\text{-onset}}$), the maximum weight loss rate temperature ($T_{d\text{-max}}$) and the corresponding weight loss of each decomposition step were summarized in Table 3. The initial weight loss of around 5 wt.% below 180 °C was due to the loss of water adsorbed in the membrane. The pure PVA membrane displayed two decomposition stages. The first broad decomposition stage ranging from 207 to 460 °C was attributed to the gradually degradation of side-groups, and the second stage after 500 °C was caused by the decomposition of the PVA cleavage backbone (or so-called carbonation) [30]. Three main weight loss stages were clearly observed for the PVA/CS membrane without doping with OPAs. The first and second sharp weight loss stages of PVA/CS membrane starting at 208 and 430 °C, respectively, with a total weight loss of 53%, were mainly ascribed to the degradation of CS chains and PVA side-groups. The third weight loss stage starting at 500 °C was mainly due to the degradation of PVA chains.

The incorporation of OPAs into the polymer matrix yielded an enhanced thermal stability with the first decomposition stage being shifted to higher temperatures by 3–34 °C compared with the undoped PVA/CS membrane. The onset temperature of the first decomposition stage ($T_{d1\text{-onset}}$) for the three kinds of OPA-doped membranes followed such an order: PVA/CS-E(13.9) > PVA/CS-H(11.2) > PVA/CS-A(12.8). The weight loss of PVA/CS-A(12.8) was higher than that of undoped PVA/CS membrane after 260 °C. The arrangement changes of PVA and CS chains occurred after the addition of ATMP led to a quicker degradation at the first step. The enhanced thermal stability of OPA-doped PVA/CS membranes was attributed to the ionic crosslinked network structure where the EDTMP and HDTMP had a much stronger crosslinking efficiency with the polymer than the ATMP did. Furthermore, the intermolecular and intramolecular hydrogen bonds also made a contribution to the enhanced thermal stability. Of these membranes, PVA/CS-E(13.9) was thermally stable up to 246 °C owing to the proper length of $-(CH_2)_n-$ chain.

3.8. Mechanical properties

The effect of doping of various OPAs on the membrane mechanical properties was investigated in terms of tensile strength and Young's modulus (data listed in Table 4). The tensile strength of the blend membranes decreased upon the addition of OPAs at a low doping content for EDTMP and HDTMP due to the destruction of the pristine orderly arrangement of polymer chains. With the increase of EDTMP and HDTMP content in the membrane, the tensile strength increased significantly, reached a level comparable to or even higher than that of the pristine PVA/CS membrane. This increasing trend was attributable to the strengthened ionic and hydrogen bond interactions between the OPAs and the polymer chains with the increase of OPA content. However, such an increasing trend was not found for ATMP-doped blend membranes where the tensile strength was lowered with the addition of ATMP. This result was in agreement with what the TG analysis proved that the ATMP exhibited a much weaker ability for crosslinking than the other two OPAs. Similar results were also found in H_3PO_4-doped membranes [13,15,19]. The reduction in elongation of the OPA-doped membranes reflected the lowered chain flexibility as a result of the enhanced crosslinking extent. All the OPA-doped mem-

Table 4
The mechanical properties PVA, PVA/CS and OPA-doped PVA/CS membranes

Membrane	OPA content (wt.%)	Elongation (%)	Tensile strength (MPa)	Young's modulus (MPa)
PVA	0	27.60	88.51	322
PVA/CS	0	12.62	85.79	680
	1.1	8.39	62.59	746
PVA/CS-A	8.4	7.85	68.29	870
	12.8	2.62	39.64	1513
	4.3	5.86	43.95	750
PVA/CS-E	10.1	10.80	84.62	784
	13.9	9.27	127.06	1370
	2.3	5.35	51.09	955
PVA/CS-H	7.7	7.99	93.22	1167
	11.2	6.72	103.23	1536

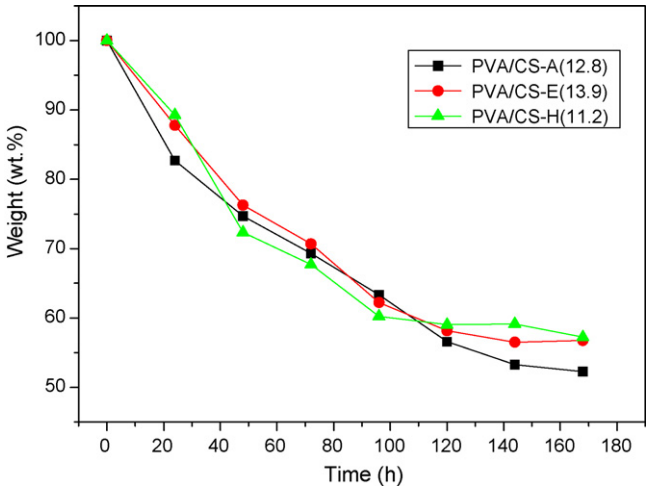

Fig. 8. The oxidative stability of OPA-doped PVA/CS membranes.

branes displayed a higher Young's modulus than the pristine PVA and PVA/CS membrane. Moreover, the Young's modulus increased with the doping content.

3.9. Oxidative stability

The oxidative stability of the OPA-doped PVA/CS membranes was evaluated by exposing the membrane to a 3 wt.% H_2O_2 solutions at 60 °C. The undoped PVA/CS membrane broke into small pieces after immersion for 24 h and completely dissolved after 48 h. For OPA-doped PVA/CS membranes, no obvious change was observed during the first 72 h, and, after 120 h, the membranes became incompact with poor mechanical strength but did not break into brittle pieces as the undoped PVA/CS membrane did. The weight loss of membranes was recorded with immersion time and shown in Fig. 8. The oxidation stability was significantly improved by incorporation of OPAs, and the three kinds of OPA-doped membranes in this study exhibited similar oxidative behavior. This strengthened oxidative stability might be attributed to the P–OH hydrogen and ionic bonds formed between –OH or $-NH_2$ and $-PO_3H_2$.

3.10. Water uptake and ion-exchange capacity

The water uptake the OPA-doped blend membranes were presented in Table 5. While the water uptake of pure PVA membrane (24.4 wt.%) was comparable to that of Nafion®117 membrane, the PVA/CS blend membrane exhibited a remarkably higher water uptake of nearly 60 wt.% owing to the high hydrophilic nature of CS and the disruption of the highly ordered arrangement of pristine PVA and CS polymer chains individually [24]. The water uptake capacity of OPA-doped PVA/CS membranes was comparable to the undoped PVA/CS membrane. The positive effect of the addition of hydrophilic OPAs and the negative effect of their crosslinking function on the water uptake seemed to reach a balance in the doping range. Since the crosslinking function of AMTP was not as strong as the other two OPAs, EDTMP and HDTMP, the water uptake of PVA/CS-A membranes was relatively higher than PVA/CS-E and PVA/CS-H membranes at similar doping contents.

Ion-exchange capacity (IEC) is an indirect and reliable approximation of the proton conductivity. The measured IEC values are shown in Table 5, The PVA and CS materials showed low IEC values due to their poor proton dissociation ability. The incorporation of OPAs led to a significant increase in IEC even at low contents. IEC values comparable to that for Nafion®117 membrane (0.78 mmol g^{-1}) were obtained by addition of only 1.1 wt.% of ATMP, 4.3 wt.% of EDTMP and 2.3 wt.% of HETMP into PVA/CS matrix. Moreover, the IEC values increased with the increase of OPA content and reached the highest level up to 1.33 mmol g^{-1} for PVA/CS-A(12.8), 1.30 mmol g^{-1} for PVA/CS-E(13.9) and 1.15 mmol g^{-1} for PVA/CS-H(11.2). This increment was a direct result of the increase in the density of $-PO_3H_2$ groups in the membrane. These high IEC values suggested high proton conductivities as discussed in the next section.

3.11. Proton conductivity

The proton conductivities of membranes were listed in Table 5 and compared with Nafion®117 membrane. The proton conductivity of Nafion®117 membrane measured at room temperature was 5.05×10^{-2} S cm^{-1} while that for PVA membrane and PVA/CS membrane was 0.10×10^{-2} and 0.97×10^{-2} S cm^{-1}, respectively. The three kinds of OPA-doped PVA/CS membranes showed a remarkably higher proton conductivity than undoped PVA/CS membrane in a range of 2.27×10^{-2} to 2.58×10^{-2} S cm^{-1}. This significant improvement in proton conductivity demonstrated the easier proton transport from acid to acid with the aid of $-PO_3H_2$ groups [9]. Moreover, the high proton conductivity was also due to the presence of zwitter ionic architecture in the OPA-doped PVA/CS blend membranes constructed by acid–base interactions and hydrogen bonds. The doping of OPAs disrupted the original orderly packing of polymer chains and gave rise to hydrophilic regions due to strong affinity toward water of –OH and $-PO_3H_2$ groups. These hydrophilic regions formed around the cluster of chains led to higher water retention and thus enable easier proton transfer [31].

Further study on the proton conductivity at elevated temperatures up to 80 °C was carried out. All the samples were well hydrated

Table 5
Water uptake, IEC, methanol permeability and proton conductivity of PVA, PVA/CS, OPA-doped PVA/CS and Nafion®117 membranes

Membrane	OPA content (wt.%)	Water uptake (wt.%)	Methanol permeability (10^{-7} cm^2 s^{-1})	IEC (mmol g^{-1})	Proton conductivity (20 ± 3 °C) (10^{-2} S cm^{-1})
Nafion®117	0	25.3	37.2	0.78	5.04
PVA	0	24.4	0.70	0.03	0.10
PVA/CS	0	59.2	2.63	0.04	0.97
	1.1	60.6	2.85	0.63	2.27
PVA/CS-A	8.4	66.3	3.43	1.15	2.64
	12.8	79.2	4.26	1.33	3.58
	4.3	65.0	2.90	0.86	2.60
PVA/CS-E	10.1	57.9	2.39	1.08	2.87
	13.9	52.3	2.32	1.30	3.51
	2.3	61.0	2.93	0.75	2.15
PVA/CS-H	7.7	56.6	2.63	1.02	2.59
	11.2	56.1	2.45	1.15	2.61

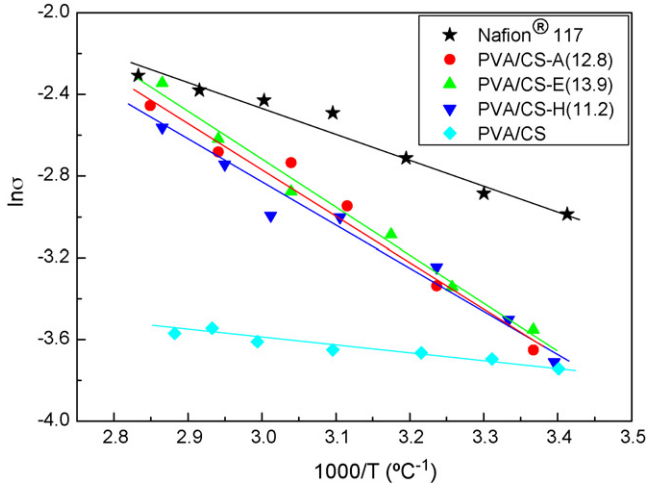

Fig. 9. Temperature dependence of proton conductivity for Nafion® 117, PVA/CS, PVA/CS-A(12.8), PVA/CS-E(13.9) and PVA/CS-H(11.2) membranes.

during the test, and eliminated the effect of humidification [32]. The change of proton conductivity with temperature agreed well with the Arrhenius law [33]. The Arrhenius plots for various membranes were presented in Fig. 9. The activation energy of proton conductivity was estimated [25] and presented in Table 6. Proton conductivity increased with the increase of temperature for all the membranes owing to the good water retainability. Two mechanisms for proton transfer were commonly adopted: Grotthus or 'hopping' mechanism and vehicle mechanism [34]. 'Hopping' mechanism refers to the proton transport through hydrogen-bonded network of water molecules and the ion-exchange sites. Vehicle mechanism refers to the coupled proton-water transport, which is strongly associated with the water content in the membrane. The activation energy of proton conductivity (E_a) for Nafion® 117 and undoped PVA/CS membranes was calculated to be 9.98 and 2.67 kJ mol^{-1}, respectively. ATMP-, EDTMP- and HDTMP-doped PVA/CS membranes presented comparable higher E_a values (16.98, 19.31 and 15.93 kJ mol^{-1}, respectively). High proton conductivities and activation energies of OPA-doped membrane were attributed to the high density of $-PO_3H_2$ groups, which provided enough sites for proton jumping from one to another. Grotthus or 'hopping' mechanism was considered to play an important role in proton transfer. Furthermore, since the O–O distance between two $-PO_3H_2$ groups in OPAs was shorter than that between two $-SO_3H$ groups in sulfonated membranes, the transport of protons along the acidic groups became easier [9]. These OPA-doped PVA/CS membranes were reasonably expected to be suitable for DMFCs operating at higher temperatures in terms of proton conductivity.

Table 6
Activation energy of conductivity of Nafion® 117, PVA/CS, PVA/CS-A(12.8), PVA/CS-E(13.9) and PVA/CS-H(11.2) membranes

Membrane	Thickness (μm)	Activation energy of conductivity (kJ mol^{-1})
Nafion® 117	190	9.98
PVA/CS	100	2.67
PVA/CS-A(12.8)	110	16.98
PVA/CS-E(13.9)	107	19.31
PVA/CS-H(11.2)	115	15.93

3.12. Methanol permeability

Methanol crossover, which occurs due to diffusion as a result of the concentration gradient and also the electro-osmotic drag is a critical problem for DMFC membranes. Decreasing methanol diffusion and correction of electro-osmotic drag effects were developed and found necessary for protonic membranes [35,36]. Herein, the methanol permeability was measured and compared based on only the diffusion behavior. The methanol permeability of the membranes prepared and Nafion® 117 at ambient temperature was shown in Table 5. The methanol permeability of pure PVA and PVA/CS membranes was 0.7×10^{-7} and 2.63×10^{-7} cm^2 s^{-1}, respectively, more than 53 and 14 times lower than that of Nafion® 117 membrane (37.2×10^{-7} cm^2 s^{-1}) [25]. This sound methanol barrier property was in accordance with other reports on separation of alcohol–water mixtures by the identical membrane materials [24,37]. The relatively higher methanol permeation of PVA/CS blend compared with pure PVA membrane was due to the disruption of the pristine highly crystalline structure of PVA by the addition of CS. The OPA-doped PVA/CS membranes retained the methanol barrier property of PVA/CS, exhibiting a methanol permeability of the same magnitude. A comparison of the three kinds of OPAs in terms of methanol permeability led to a conclusion that EDTMP- and HDTMP-doped membranes showed better methanol barrier properties than ATMP-doped membranes. A lower crystallinity or a higher content of amorphous phases and a less compact crosslinking structure usually result in a bigger alcohol crossover. For the EDTMP- and HDTMP-doped membranes, the diminishment of crystalline regions caused by the doping of OPAs were compensated by the construction of the crosslinking structure formed between the OPA molecules and the polymer via both acid–base interaction and hydrogen bonds. As a result, the methanol barrier property could be well retained. For ATMP, the crosslinking function was much weaker compared to the other two OPAs probably due to its smaller molecular size and lower content of acid groups. Therefore, the ATMP-doped membranes exhibited higher methanol permeability and this methanol permeability became even more severe with the increase of doping content. This tendency was in accordance with the water uptake of the membranes since the methanol permeation was positively related to swelling behavior. In addition, the length of $-(CH_2)_n-$ chains between the phosphonic acid groups also influenced the crosslinking degree. In this study, the PVA/CS membrane doped with EDTMP with moderate $-(CH_2)_2-$ chain length showed the best performance in terms of both proton conductivity and methanol barrier property.

4. Conclusions

A novel series of OPA-doped PVA/CS membranes was fabricated by blending the PVA and CS aqueous mixture with three OPAs including ATMP, EDTMP and HDTMP to increase the proton conductivity without sacrificing the methanol barrier property. The characterization studies with FT-IR, XRD, XPS and TGA and the evaluation for membrane performance confirmed the dual function of OPAs exerting in the membrane: (1) proton conductor: a high proton conductivity of about 3.5×10^{-2} S cm^{-1} was achieved for OPA-doped PVA/CS membranes, comparable with that for Nafion® 117 membrane (5.04×10^{-2} S cm^{-1}); (2) crosslinker: a dense structure of OPA-doped membrane was achieved through acid–base ionic interactions and hydrogen bonds. Meanwhile, low methanol permeability values around 3×10^{-7} cm^2 s^{-1} for OPA-doped PVA/CS membranes, one order of magnitude lower than that of Nafion® 117 membrane, were obtained. The above proper-

ties as well as the sound mechanical strength render the OPA-doped membranes promising application potential in DMFCs.

Acknowledgements

We gratefully acknowledge financial support from the National Nature Science Foundation of China (No.: 20776101), the Programme of Introducing Talents of Discipline to Universities (No.: B06006), the National Basic Research Program of China (No.: 2008CB617502) and the Cross-Century Talent Raising Program of Ministry of Education of China. We thank Professor Yuxin Wang for his help in the proton conductivity measurements.

References

[1] V. Neburchilov, J. Martin, H. Wang, J. Zhang, J. Power Sources 169 (2007) 221–238.
[2] Y. Yang, Z. Shi, S. Holdcroft, Macromolecules 37 (2004) 1678–1681.
[3] S. Zhong, X. Cui, H. Cai, T. Fu, C. Zhao, H. Na, J. Power Sources 164 (2007) 65–72.
[4] C.H. Lee, C.H. Park, Y.M. Lee, J. Membr. Sci. 313 (2008) 199–206.
[5] Y. Shen, X. Qiu, J. Shen, J. Xi, W. Zhu, J. Power Sources 161 (2006) 54–60.
[6] J. Choi, D.H. Kim, H.K. Kim, C. Shin, S.C. Kim, J. Membr. Sci. 310 (2008) 384–392.
[7] Y.T. Hong, C.H. Lee, H.S. Park, K.A. Min, H.J. Kim, S.Y. Nam, Y.M. Lee, J. Power Sources 175 (2008) 724–731.
[8] J.A. Kerres, Fuel Cells 5 (2) (2005) 230–247.
[9] S.J. Paddison, K.D. Kreuer, J. Maier, Phys. Chem. Chem. Phys. 8 (2006) 4530–4542.
[10] M. Yamada, I. Honma, Polymer 46 (2005) 2986–2992.
[11] T. Itoh, K. Hirai, M. Tamura, T. Uno, M. Kubo, Y. Aihara, J. Power Sources 178 (2008) 627–633.
[12] S. Li, Z. Zhou, M. Liu, W. Li, J. Ukai, K. Hase, M. Nakanishi, Electrochim. Acta 51 (2006) 1351–1358.
[13] Y. Zhai, H. Zhang, Y. Zhang, D. Xing, J. Power Sources 169 (2007) 259–264.
[14] Q. Li, R. He, J.O. Jensen, N.J. Bjerrum, Chem. Mater. 15 (2003) 4896–4915.
[15] J. Lobato, P. Cãnizares, M.A. Rodrigo, J.J. Linares, J.A. Aguilar, J. Membr. Sci. 306 (2007) 47–55.
[16] Y.S. Kim, F. Wang, M. Hickner, T.A. Zawodzinski, J.E. McGrath, J. Membr. Sci. 212 (2003) 263–282.
[17] M.L. Ponce, L. Prado, B. Ruffmann, K. Richau, R. Mohr, S.P. Nunes, J. Membr. Sci. 217 (2003) 5–15.
[18] S.Ü. Celik, A. Bozkurt, Eur. Polym. J. 44 (2008) 213–218.
[19] P.R. Sukumar, W. Wu, D. Markova, Ö. Ünsal, M. Klapper, K. Müllen, Macromol. Chem. Phys. 208 (2007) 2258–2267.
[20] H. Steininger, M. Schuster, K.D. Kreuer, J. Maier, Solid State Ionics 177 (2006) 2457–2462.
[21] V.V. Binsu, R.K. Nagarale, V.K. Shahi, P.K. Ghosh, React. Funct. Polym. 66 (2006) 1619–1629.
[22] C.W. Lin, R. Thangamuthu, C.J. Yang, J. Membr. Sci. 253 (2005) 23–31.
[23] P. Mukoma, B.R. Jooste, H.C.M. Vosloo, J. Membr. Sci. 243 (2004) 293–299.
[24] B. Smitha, S. Sridhar, A.A. Khan, J. Appl. Polym. Sci. 95 (2005) 1154–1163.
[25] Z. Jiang, X. Zheng, H. Wu, J. Wang, Y. Wang, J. Power Sources 180 (2008) 143–153.
[26] D. Hofmann, L. Fritz, J. Ulbrich, C. Schepers, M. Böhning, Macromol. Theory Simul. 9 (2000) 293–327.
[27] F. Pan, F. Peng, Z. Jiang, Chem. Eng. Sci. 62 (2007) 703–710.
[28] W. Yuan, H. Wu, B. Zheng, X. Zheng, Z. Jiang, J. Power Sources 172 (2007) 604–612.
[29] L. Lu, H. Sun, F. Peng, Z. Jiang, J. Membr. Sci. 281 (2006) 245–252.
[30] C.C. Yang, J. Membr. Sci. 288 (2007) 51–60.
[31] K. Miyatake, K. Oyaizu, E. Tsuchida, A.S. Hay, Macromolecules 34 (2001) 2065–2071.
[32] X. Ren, M.S. Wilson, S. Gottesfeld, J. Electrochem. Soc. 143 (1996) L12–L15.
[33] C.W. Lin, Y.F. Huang, A.M. Kannan, J. Power Sources 171 (2007) 340–347.
[34] B.S. Pivovar, Y. Wang, E.L. Cussler, J. Membr. Sci. 154 (1999) 155–162.
[35] X. Ren, T.E. Springer, T.A. Zawodzinski, S. Gottesfeld, J. Electrochem. Soc. 147 (2000) 466–474.
[36] B.S. Pivovar, W.H. Smyrl, E.L. Cussler, J. Electrochem. Soc. 152 (2005) A53–A60.
[37] S.K. Dae, B.P. Ho, W.R. Ji, M.L. Young, Solid State Ionics 176 (2005) 117–126.